

Supporting information to “Internal Photoemission (IPE) in Molecular Junctions: Parameters for Interfacial Barrier Determinations”

Supporting Information For: “Internal Photoemission in Molecular Junctions: Parameters for Interfacial Barrier Determinations”

Jerry A. Fereiro¹, Mykola Kondratenko^{1,2}, Adam Johan Bergren^{*2}, Richard L. McCreery^{*1,2}

¹Department of Chemistry, University of Alberta, Edmonton, AB

²National Institute for Nanotechnology, National Research Council Canada

*Correspondence to: adam.bergren@nrc.ca (AJB), richard.mccreery@ualberta.ca (RLM);

Introduction

This document contains additional supporting data, figures, discussions, and equations used to support the main text. Specifically:

1. Schematic representation of the junction structure.
2. Molecular structures.
3. Experimental apparatus: Modulated source apparatus and DC laser source measurements.
4. Method for determining the absorption spectra of molecular layers.
5. Optical absorption spectra and determining the onset of optical absorption.
6. Excitation-intensity profiles for alkanes and related analysis for multiple molecules.
7. Optical absorption spectra of Fc and NDI molecule with their structures.
8. Yield vs. molecular thickness plot AB, NAB, NDI and Fc.
9. Fowler plots.

1. Schematic representation of the junction structure:

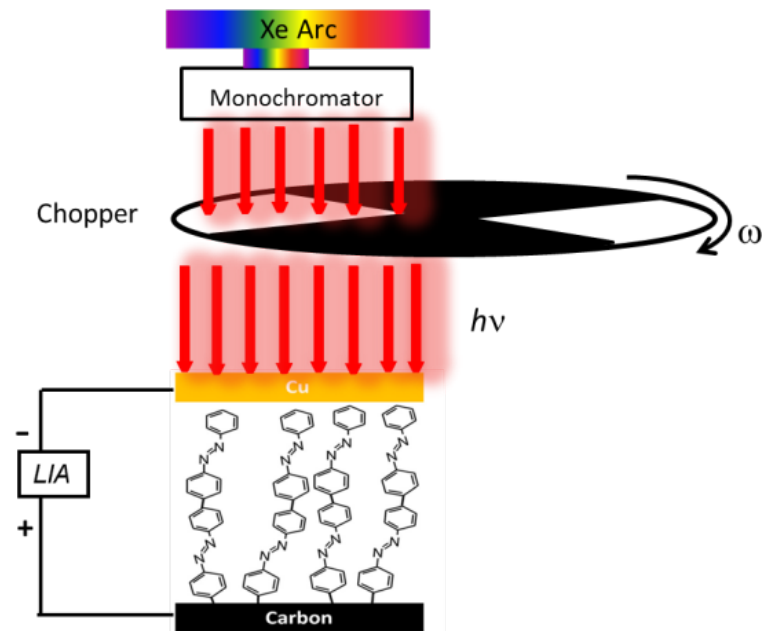


Figure S1: Schematic representation of the junction structure.

Figure S1 shows the schematic of the junction structure used in this study. Details of junction fabrication¹ and the photocurrent measurement can be found in the supporting information of a previously published paper². Briefly, a narrow band ($\Delta\lambda=13\text{nm}$) of light from a xenon arc source (Newport model 6256) passes through an optical chopper before incidence onto the top of a molecular junction. A dual phase LIA is used to measure both the phase and the magnitude of the photocurrent simultaneously.

2. Molecular Structures:

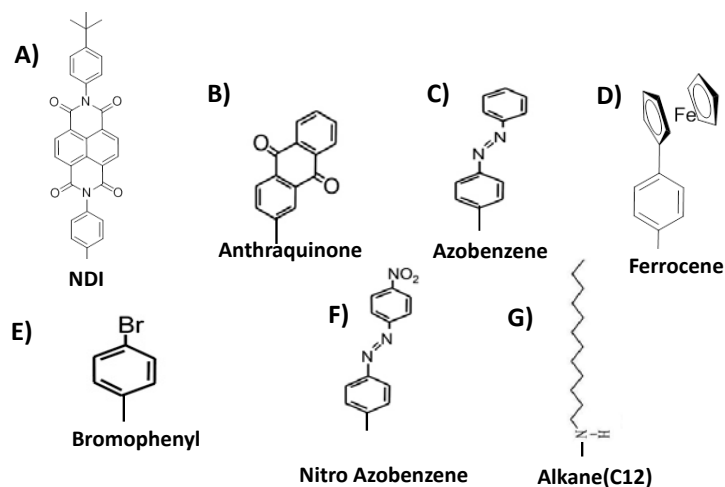


Figure S2: The structures of all the molecules used in this study. (A) NDI; (B) Anthraquinone; (C) Azobenzene; (D) Ferrocene; (E) Bromophenyl; (F) Nitroazobenzene; (G) Alkane (C₁₂H₂₅N). In most cases, molecular layers were multilayers of several molecules, with thicknesses indicated in main text.

3. Experimental apparatus:

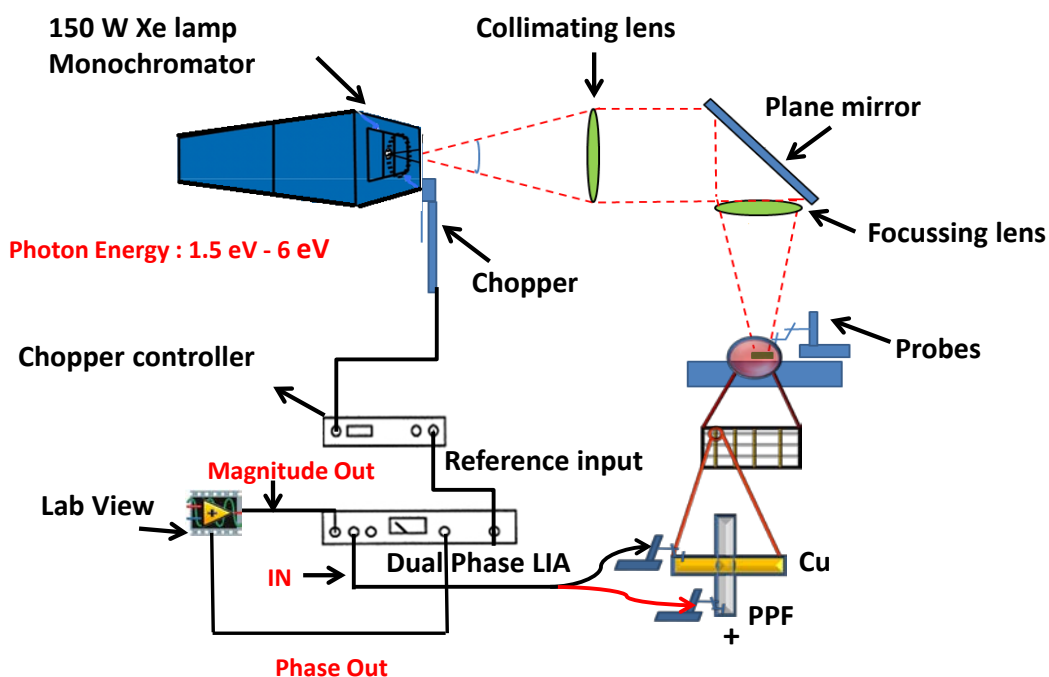


Figure S3-A: Apparatus with Xe arc continuum source, modulation by an optical chopper and detection with a Lock-In -Amplifier (LIA).

Supporting information to “Internal Photoemission (IPE) in Molecular Junctions: Parameters for Interfacial Barrier Determinations”

Figure S3-A shows a diagram of the experiment using a 150 W Xenon arc lamp (Newport model 6256) as the source of illumination. After passing through a Newport model 74004 Cornerstone 130 1/8 m motorized monochromator (band pass = 13 nm), the selected wavelength was chopped at frequency ω (typically 400 Hz). The chopped light was then directed through a series of lenses and mirrors for focusing. The PPF contact was connected via a tungsten probe and shielded cable to the AC-coupled current input of a dual phase lock-in amplifier (LIA, Stanford-830), and the shield (ground) was connected to the Cu contact of the molecular junction. The output from the LIA was recorded using a Labview data acquisition program. In all cases, the PPF was considered the positive terminal, as shown in Figure S3A.

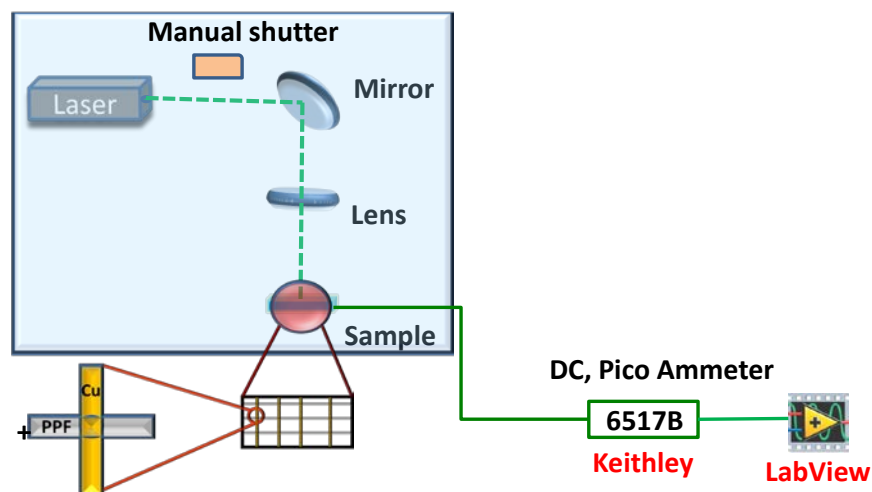


Figure S3-B: Laser experimental apparatus for DC illumination and photocurrent measurement

Figure S3-B shows the diagram of the apparatus using argon ion (458 nm/2.7 eV, and 514 nm/2.4 eV), krypton ion (675 nm/1.8 eV), and a diode lasers (780 nm/1.58 eV) as sources of illumination. The wavelength of the monochromatic laser source before each experiment was

Supporting information to “Internal Photoemission (IPE) in Molecular Junctions: Parameters for Interfacial Barrier Determinations”

verified using an Ocean Optics spectrometer (USB-4000). The power from the laser beam at the sample was determined using a power meter directly above the sample before and after each experiment. For all the experiments carried out in this study, the intensity of the laser beam was varied between 1 and 50 mW, with a focused spot size of ~1 mm. A manual shutter was used to control exposure time. The PPF contact was contacted with a tungsten probe and connected to the input of a DC picoammeter (Kiethley 6517B) to read the photocurrent, and the output from the picometer was recorded using a Labview data acquisition program. 808 nm and 852 nm Fabry-Perot laser diodes from Thorlabs were capable of 100 mW output each. A Thorlabs LDC 210C laser diode controller and a TED 200C thermoelectric temperature controller were used to drive and control laser output.

4. Method for determining Absorption spectra

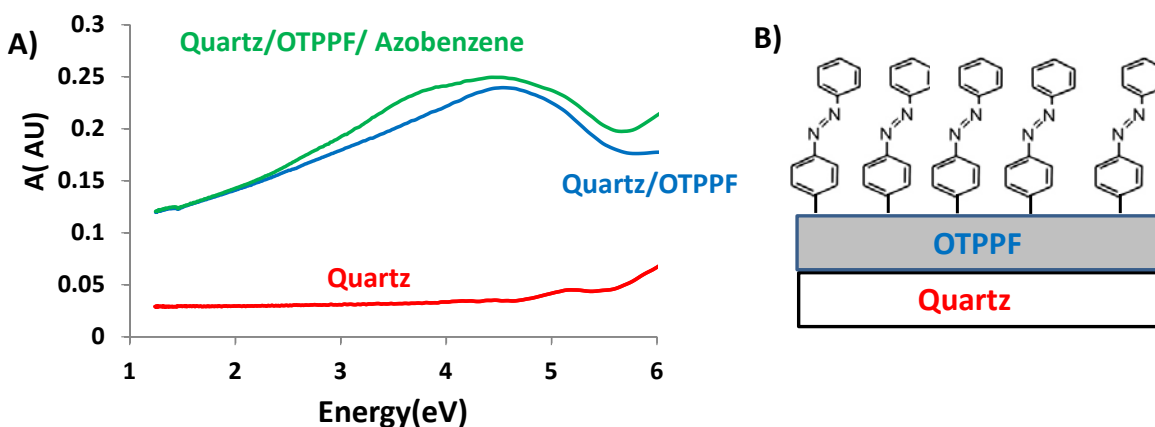


Figure S4-A: Absorption spectra of quartz (red) only, Quartz with optically transparent photoresist film (OTPPF-blue) and finally the Quartz/OTPPF surface modified with azobenzene to make Quartz/OTPPF/Azobenzene (green). **B:** Schematic representation of the junction.

Polished quartz wafers (Technical Glass Products, Inc.) were diced into 1.2 x 1.5 cm chips to serve as substrates. The substrates were initially cleaned by sonication in acetone, IPA, and water for 10 minutes each^{1,3}. After sonication, the cleaned quartz substrates were dried using a stream

Supporting information to “Internal Photoemission (IPE) in Molecular Junctions: Parameters for Interfacial Barrier Determinations”

of N₂ gas. The absorption spectra of each quartz substrate (with an air reference) were obtained using a Perkin Elmer 900 spectrometer. The red curve in Figure S4-A shows the absorbance of a typical quartz substrate. After obtaining the spectrum for each quartz substrate, a commercially-available photoresist (AZ-P4330-RS) was diluted (5 % by volume) using propylene glycol methyl ether acetate, then this solution was spin coated onto quartz slides at 6000 rpm for 60 sec⁴. After soft baking at 90°C for 10 min, samples were transferred to a tube furnace for pyrolysis. Forming gas (5% H₂ in N₂) was kept flowing at 100 sccm throughout pyrolysis, during which the temperature was ramped at 10° C/min up to 1025 °C for 1 hour, as reported elsewhere^{3,4}, resulting in an optically-transparent pyrolyzed photoresist film. The absorption spectra of the optically transparent PPF (OTPPF) films were then obtained, with a typical result shown in Figure S4-A, blue curve. Finally the OTPPF substrate was modified with molecular layers ranging from 1 to 5 nm in thickness using electrochemical reduction of diazonium salts in solution as reported elsewhere⁴. An example of the absorbance spectrum obtained for a layer of azobenzene on OTPPF is shown in Figure S4-A, green curve. Figure S4-A shows all three absorption curves for each component of the sample taken at different times during fabrication. Figure S4-B shows a schematic of a completed sample.

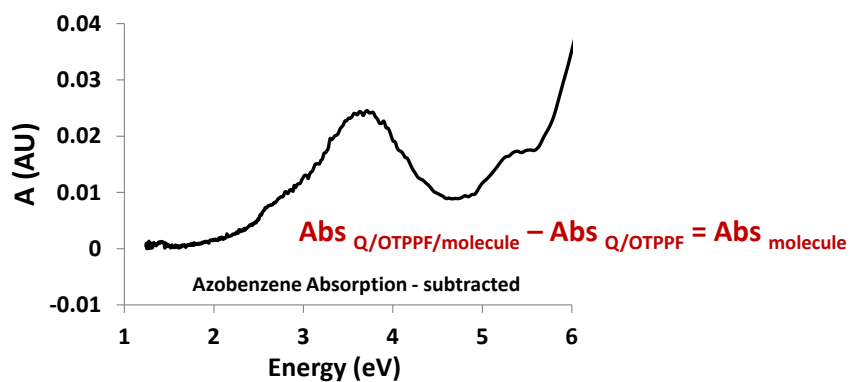


Figure S4-C: Absorption spectrum of Azobenzene (3.4 nm) obtained from the spectra of figure S4A.

In order to obtain the absorption spectrum for a molecular layer, the absorbance obtained from an unmodified quartz/carbon substrate (described above) is subtracted from that for the same sample following modification by the molecular layer (i.e., quartz/OTPPF/AB). The result is shown in Figure S4-C. The small negative absorbance is due to the refractive index change between the reference (unmodified transparent carbon) and the sample upon addition of the thin molecular layer.

5. Optical absorption spectra for different molecules:

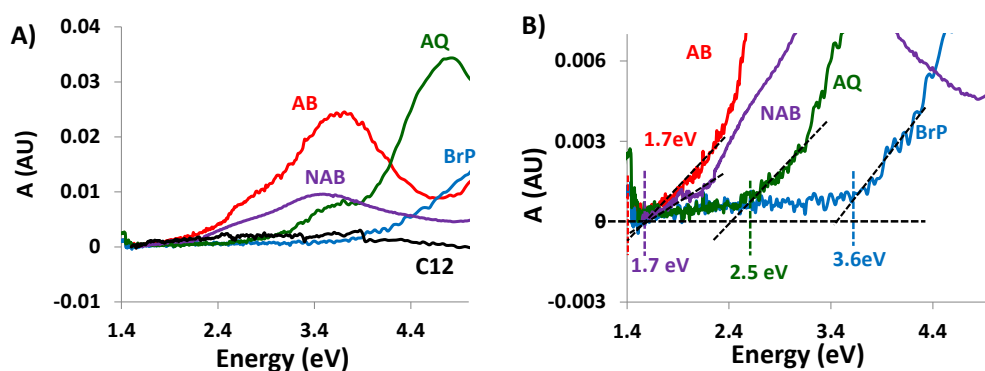


Figure S5-A: Optical absorption spectra C12, AQ, AB, NAB, and BrP following subtraction of OTPPF spectrum. **B:** Method for determining onset of optical absorption.

Figure S5-A shows the overlay of optical absorption spectra for the different molecules used in this study using the procedure outlined above. The onset of absorption by molecular layer is taken as the intersection of two linear regions of the corrected spectrum as shown in figure S5B. The optical absorption onset for thus determined was 1.7 eV (AB and NAB), 2.5 eV (AQ) and 3.6eV (BrP, as reported in the main text Table 1).

6. Excitation intensity profiles for alkanes:

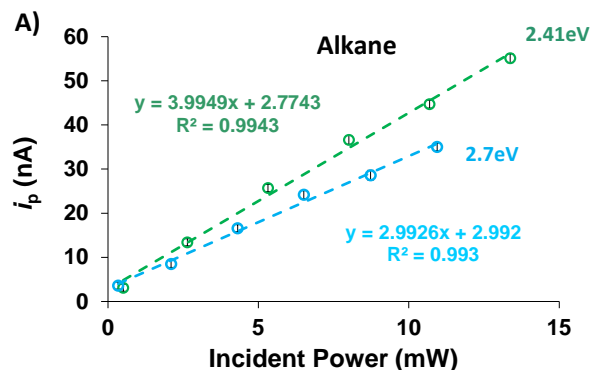


Figure S6: Photocurrent vs. intensity for an alkane junction at 2.4 eV (458 nm) and 2.7 eV (516 nm).

Figure S6 shows the photocurrent as a function of excitation intensity for alkane junctions for two different energies (2.4 and 2.7 eV). The linearity of the curves shows that the photocurrent is controlled by monomolecular recombination.

Table S1 lists the correlation coefficient (R^2) determined from linear (I_{photo} vs. Intensity) or quadratic [$(I_{\text{photo}})^2$ vs Intensity] plots of photocurrent vs incident light intensity in Watts. NDI, Fc, BrP, AQ and alkane junctions more closely fit a linear function of intensity at 2.7 and 2.4 eV, while AB has a better fit to a quadratic function at either 2.4 or 1.9 eV. Photocurrent vs. intensity curves for the alkane are in Figure S6, and those for all other molecules are provided in the main text.

Supporting information to “Internal Photoemission (IPE) in Molecular Junctions: Parameters for Interfacial Barrier Determinations”

NDI			Fc		
Graph	R ² fitting value (2.7eV)	R ² fitting Value (2.4eV)	Graph	R ² fitting value (2.4eV)	R ² fitting Value (1.9eV)
I _{photo} Vs incident power	0.9899	0.9893	I _{photo} Vs incident power	0.9966	0.9967
(I _{photo}) ² Vs incident power	0.9552	0.9819	(I _{photo}) ² Vs incident power	0.944	0.9073

BrP			AB		
Graph	R ² fitting value (2.4eV)	R ² fitting Value (2.7eV)	Graph	R ² fitting value (2.4eV)	R ² fitting Value (1.9eV)
I _{photo} Vs incident power	0.9917	0.9946	I _{photo} Vs incident power	0.9638	0.9653
(I _{photo}) ² Vs incident power	0.9646	0.9696	(I _{photo}) ² Vs incident power	0.998	0.9937

AQ			Alkane		
Graph	R ² fitting value (2.4eV)	R ² fitting value (1.8eV)	Graph	R ² fitting value (2.4eV)	R ² fitting Value (2.7eV)
I _{photo} Vs incident power	0.9952	0.9981	I _{photo} Vs incident power	0.9943	0.993
(I _{photo}) ² Vs incident power	0.9314	0.9728	(I _{photo}) ² Vs incident power	0.9646	0.9692

Table S1: R² correlation coefficient for both I_{photo} vs. incident power and the (I_{photo})² vs. the incident power for all molecular junctions in this study.

7. Structure and absorption spectra for NDI and ferrocene molecular layers:

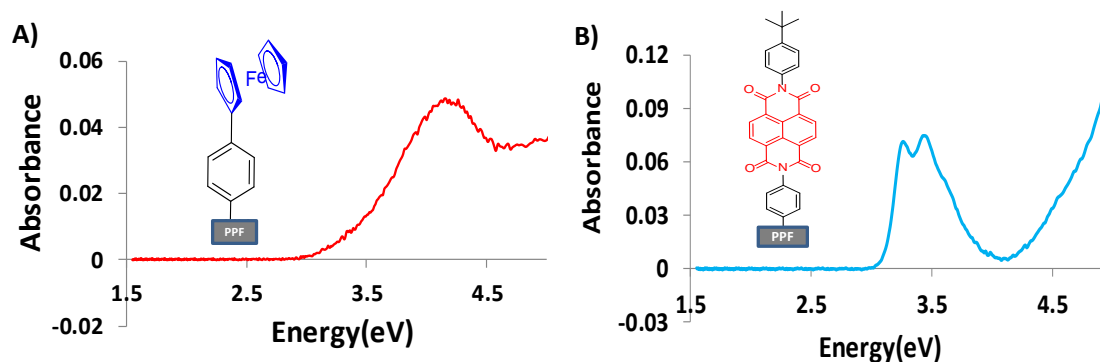


Figure S7: Absorption spectra of Fc (A) and NDI (B) films on OTPPF (both NDI & Fc are 3-4nm thick), after subtraction of the OTPPF spectrum

Figure S7-A shows the optical absorption spectrum for Ferrocene (Fc) with an inset showing schematic structure of Fc molecule on the carbon surface. Figure S8-B shows the optical absorption spectrum of NDI with inset showing its structure. The optical absorption spectrum for each molecule was obtained from the procedure of section 4 above.

8. Yield vs. molecular layer thickness plots:

Yield vs. molecular layer thickness plots for AB, NAB, NDI and Fc are shown in figure S8. As noted in the main text, the thickness dependence is much larger when the molecular layer absorbs light.

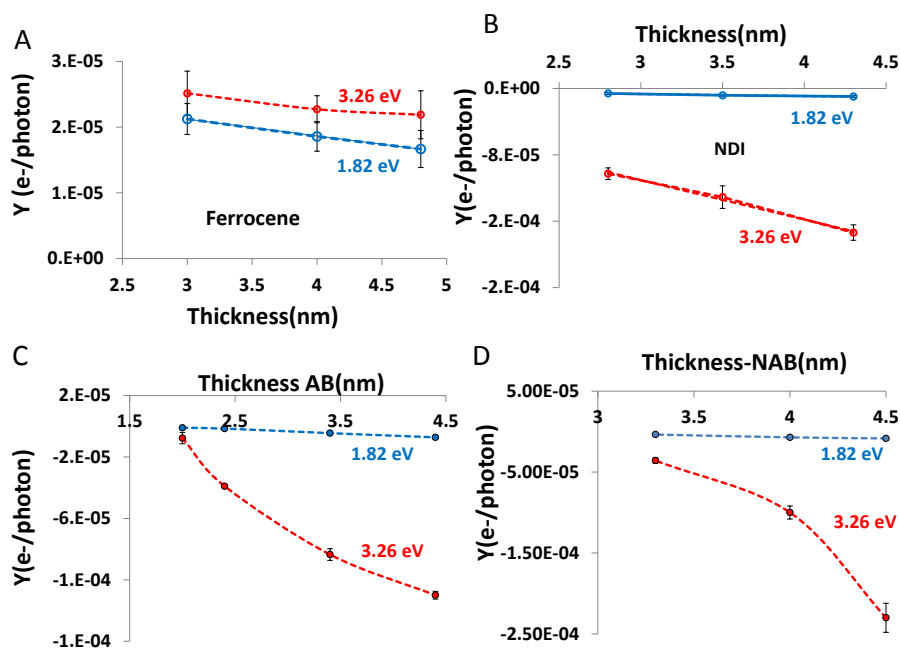


Figure S8: Yield vs. thickness plot of Fc, NDI, AB and NAB used in the study

9. Fowler Plots:

Figure S9 shows the Fowler plots for all the molecules studied. The error bars show the standard deviation of photocurrent for four different junctions on the same sample. Table S2 shows the value of Fowler intercepts obtained from the Fowler plots, and they are provided in the main text, table 2 The intercepts and their errors were determined statistically using standard methods⁵ as follows. Let x_i represent photon energy y_i represent $Y^{1/2}$, A the y-axis intercept of the $Y^{1/2}$ vs. photon energy plot, B the associated slope, and σ_A the error of the intercept on the ordinate.

$$A = \frac{\sum x^2 \sum y - \sum x \sum xy}{\Delta} \quad (S1)$$

$$B = \frac{N \sum xy - \sum x \sum y}{\Delta} \quad (S2)$$

$$\Delta = N \sum x^2 - (\sum x)^2 \quad (S3)$$

$$\sigma_y = \sqrt{\frac{1}{N-2} \sum_{i=1}^N (y_i - A - Bx_i)^2} \quad (S4)$$

$$\sigma_A = \sigma_y \sqrt{\frac{\sum x^2}{\Delta}} \quad (S5)$$

$$\sigma_B = \sigma_y \sqrt{\frac{N}{\Delta}} \quad (S6)$$

The Fowler intercept on the photon energy axis is the absolute value of A/B , and the error on this intercept (σ_{Fowler}) is determined by equation S7.

$$\sigma_{Fowler} = \left| \frac{A}{B} \right| \left(\frac{\sigma_B}{|B|} + \frac{\sigma_A}{|A|} \right) \quad (S7)$$

The values obtained from this equation are given in table S2:

Supporting information to “Internal Photoemission (IPE) in Molecular Junctions: Parameters for Interfacial Barrier Determinations”

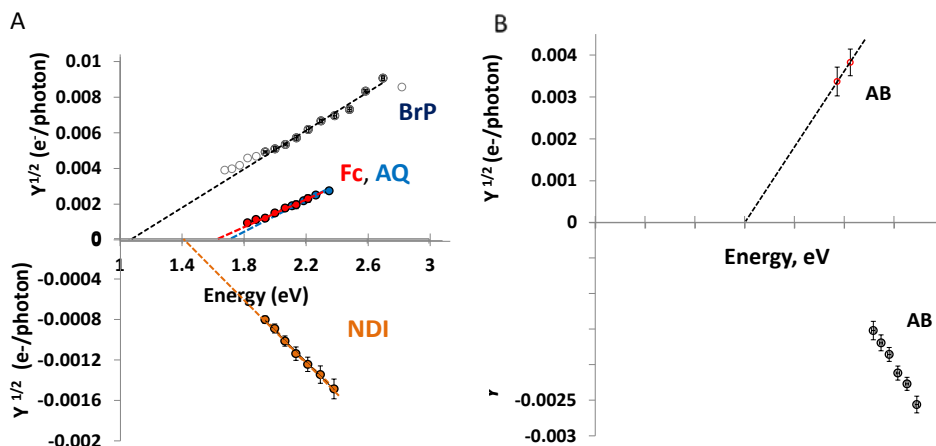


Figure S9: Fowler plots for BrP, NDI, Fc, AQ and AB.

Junction	Fowler intercept	σ_{Fowler}
BrP (3.0nm)	1.10 eV	0.11 eV
AQ (3.3nm)	1.65 eV	0.10 eV
AB ^a (3.4nm)	0.9eV	-
NAB ^b (3.3nm)	<1.4eV	-
Fc (4.0nm)	1.60eV	0.15 eV
NDI (3.5nm)	1.40eV	0.30 eV

Table S2: Fowler intercepts for each molecule along with their errors.

- a- Approximate, based on two points (808 and 852 nm), insufficient data points to calculate the error for intercept.
- b- NAB does not meet the criteria for IPE; therefore the Fowler intercept is not relevant.

References

- (1) Ranganathan, S.; McCreery, R. L. *Anal. Chem.* **2001**, *73*, 893.
- (2) Fereiro, J. A.; McCreery, R. L.; Bergren, A. J. *Journal of the American Chemical Society* **2013**, *135*, 9584.

Supporting information to “Internal Photoemission (IPE) in Molecular Junctions: Parameters for Interfacial Barrier Determinations”

- (3) Ranganathan, S.; McCreery, R. L.; Majji, S. M.; Madou, M. J. *Electrochem. Soc.* **2000**, *147*, 277.
- (4) Tian, H.; Bergren, A. J.; McCreery, R. L. *Applied Spectroscopy* **2007**, *61*, 1246.
- (5) Taylor, J. R. *An Introduction to Error Analysis: The Study of Uncertainties in Physical Measurements*; 2nd ed.; University Science Books: Sausalito, California, 1997, pp. 182-190